

# Study on stress variation law of hard concretion coal under the action of pick based on DYNA

Xunan Liu <sup>a</sup>, Yanpeng Zhang <sup>a</sup>, Jie Wang <sup>a</sup>, Hongye Li <sup>a</sup> & Lianwei Ma <sup>b</sup>

<sup>a</sup> School of Mechanical Engineering, Liaoning Technical University, Fuxin, China. yuwuknan@163.com, 1076576234@qq.com, sunny\_jiewang@163.com, Corresponding author: apple\_lxn@163.com

<sup>b</sup> CCTEG Taiyuan Research Institute, Taiyuan, Shanxi, China. mhw6916@163.com

Received: February 3<sup>rd</sup>, 2023. Received in revised form: April 27<sup>th</sup>, 2023. Accepted: May 31<sup>th</sup>, 2023

## Abstract

Modeling and simulation of pick cutting hard concretion coal process are taken as a key link to analyze the stress variation law. To this aim, the properties of hard concretion coal in the target mining area were tested. Related model with high-quality common grid was generated using the mapping method through Hypermesh. The coal breaking process was performed using LS-DYNA, and the stress variation law of coal and hard concretion was analyzed. The results showed that the closer the action position to the middle point of long axis of hard concretion, the greater stress peak would be generated, stripping of the pick occurred when it acted on the 2/5 and 1/2 positions of the long axis. Using similarity theory, the model of hard concretion coal was made and the pick cutting experiment was performed. Compared with simulation torque result, the correctness of modeling and simulation has been verified.

**Keywords:** hard concretion; coal; finite element analysis; stress variation law; similarity theory

# Estudio sobre la ley de variación del estrés del carbón de concreción dura bajo la acción del pico basado en DYNA

## Resumen

El modelado y la simulación durante el corte de hulla son elementos clave para analizar las leyes de variación de las tensiones. Con este fin, se realizaron pruebas de rendimiento de carbón duro de la mina objetivo. Generación de modelos correlacionados con mallas comunes de alta calidad utilizando el método de mapeo de Hypermesh. LS-DYNA ha sido utilizado para analizar las fracturas de pico de carbón y las tensiones en el carbón y el hormigón. Los resultados muestran que cuanto más cerca del centro del eje mayor sea el pico de tensión. Los bloques duros se desprenden cuando hachas se encuentran en 1/2 y 2/5 del eje mayor. Se ha desarrollado un modelo de carbón endurecido utilizando la teoría de la similitud y se ha realizado un experimento de corte por pico. La corrección del modelado y la simulación se verificó mediante la comparación con los resultados de simulación.

**Palabras clave:** concreción dura; carbón; análisis de elementos finitos; ley de variación de estrés; teoría de la similitud

## 1 Introduction

China has achieved leading technical levels in the mining of medium and thick coal [1], but there are still difficulties in mining thin coal and complex coal seams. These seams have limited mining space, and manual operations are difficult, leading to low mining efficiency and insufficient economic returns, resulting in the abandonment of thin coal seams [2,3]. Thin coal seams contribute only 10.4% to the total output of coal mining [4], and their mining conditions are

depicted in Fig. 1.

Thin coal seams often contain hard concretions, leading to significant stress changes in the coal seam during mining. The distribution of stress affects the collapse patterns of coal and hard concretion. By studying the rules governing coal stress changes and the forms of hard concretion breakdown when cutting teeth act on different positions of the hard concretion, it is possible to reduce energy consumption during the cutting process and minimize the impact of hard concretion on cutting teeth. This can improve the stability

and reliability of coal mining machines, and has important academic significance and engineering implications. Therefore, scholars both domestically and abroad have conducted extensive research on this topic.

British scholars Evans et al. [5,6] have researched the sharp knife cut tooth broken rock theory and passivation of the knife cut teeth rock damage theory. They proposed that the pick applies compressive stress on the surrounding coal and rock, forming an arc fracture line with the increase of compressive stress, which then causes tensile failure of coal and rock. They obtained the mechanical model of peak cutting force during coal and rock fracture. Wang QK [7], a former Soviet Union scholar, elaborated on the theory of coal breaking by shearer and experimentally verified it. Liu [8] proposed the accumulation algorithm covering the total number of curve boxes, and clearly defined the physical meaning of evaluating the fractal dimension and other characteristic quantities of the cutting resistance curve. Wang [9] conducted a simulation of cutting coal walls using a self-made test bench and monitored the cutting force. Turkish scholar Yilmaz et al. [10] predicted the cutting force of hard rock cut by the pick, establishing the relationship between cutting force and various factors. They also provided the calculation method and theoretical formula of hard rock cutting force for a crushing compressive strength of the pick ranging from 85 to 180 MPa. Wang [11] developed a coal-rock cutting experimental platform and collected stress data from the roof and floor. Bakar [12] simulated the process of cutting coal and rock using shearer teeth, while Luo [13] established a mechanical model for cutting homogeneous coal strata and coal-bearing rock sections with pick cutters and roller rotators.

Due to the complexity of shearer cutting technology and the challenging working environment, it is difficult to conduct underground experiments. However, numerical simulations are low-cost and can generate multiple sets of data in a short period, making them easy to perform. Therefore, they provide a basis for studying the stress distribution law of coal rock with hard concretion fractures.



Figure 1. Site of coal mining.

Source: Yangcun Mine, Yanzhou Mining Area, Shandong Province, 2020.

Zhao and Dong [14] conducted simulations of three loads of drum shearer using ADAMS and verified the results with theoretical formulas. He [15] used LS-DYNA to simulate the coal breaking process of the drum shearer and analyzed the relationship between the dynamic change of the plastic domain of coal seam and stress distribution. Wyk [16] performed a finite element analysis by comparing the cutting process of picks with different shapes, while keeping the cutting speed of the coal seam constant, and found that the stress of the picks is affected by the feed force and the tool wear history. Zhang [17] used FLAC3D to analyze the stress distribution of coal and rock under different mining rates and concluded that the stress distribution of coal and rock exhibits a two-stage characteristic, with the maximum concentration value acting as the cut-off point. Liu [18] utilized the finite element method to investigate the stress distribution of coal seams under the influence of picks with different structural parameters. Zhou [19] established a coal-rock coupling model of the spiral drum using LS-DYNA software under complex coal seam conditions and analyzed the stress of broken gangue coal and rock. Liu [20] established a coupling model of a screw drum for cutting gangue coal and rock using LS-DYNA, and studied the variation in the maximum stress of coal and rock under different kinematic parameters. Liu [21] simulated the process of a disc cutter crushing coal and rock using ABAQUS and analyzed the stress distribution of coal and rock under different cutting thicknesses. Menezes et al. [22] utilized the finite element method to simulate the interaction between the cutter and rock. They investigated the cutting process of rock with different cutting depths and speeds and derived the rock breaking law. Wang [23] employed ABAQUS to simulate the rock breaking process of hob crushing coal and rock. He analyzed the stress changes of coal and rock under various kinematic parameters. Liu [24] calculated the elastic energy based on SHPB dissipation energy, studied the energy release characteristics of coal and rock under different initial stress levels and strain rates, and explored the impact of energy release on rock breakage.

The scholars mentioned above have used different methods to simulate the cutting process of picks and have obtained reliable data and conclusions through analysis. This verifies that the numerical simulation method is effective in simulating the coal breaking process, thus laying a foundation for the study of the stress distribution law of coal with hard concretion broken by picks.

In addition, numerous studies have been performed on homogeneous coal rocks, while only a few scholars have researched stratified coal rocks. In the mining of thin coal seams, the equipment is more affected by induration, which impacts its reliability. If we can define the grid and contact problems of hard concretion and coal seam reasonably, simulate various cutting conditions, and analyze the stress of the hard concretion coal seam when it breaks, it will aid in reducing energy consumption during the cutting process, minimizing impact, and ultimately enhancing the reliability of the entire machine. This has great theoretical guiding significance for efficient and environmentally friendly mining of hard concretion coal.

## 2 Establishment of 3D model for cutting hard concretion coal with pick

### 2.1 Determination of mechanical parameters of hard concretion and coal

To ensure the accuracy and reliability of the numerical simulation results, it is important to consider the impact of coal and concretion properties, as well as the shape and size differences of hard concretions when establishing the coal seam model. In this study, samples of coal from the 17th layer of Yangcun Mine in the Yanzhou mining area, Jining City, Shandong Province (China), were collected and tested for their physical and mechanical properties. The results are presented in Fig. 2, and the physical and mechanical property parameters of coal and hard concretion are summarized in Table 1 and Table 2, respectively.

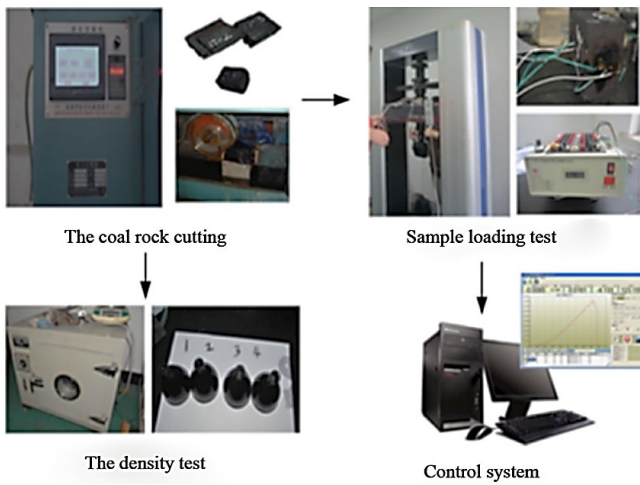


Figure 2. Mechanical property test.  
Source: Experimental acquisition, 2020.

Table 1.  
Physical and mechanical properties of coal.

Parameter	#1	#2	#3	Average
Density/(kg)m <sup>-3</sup>	3320	3056	2915	3097
Elastic modulus /GPa	15	14.6	14.8	14.8
Poisson's ratio	0.18	0.18	0.18	0.18
Cohesion/MPa	13.2	13.8	13.6	13.4
Internal friction Angle /(°)	48	47	49	48
Compressive strength /MPa	80.2	88.9	74.3	81.1
Coefficient of firmness f	8.0	8.8	7.4	8.1

Source: Experimental acquisition, 2020.

Table 2.  
Parameters of coal and hard concretion.

Parameter	#1	#2	#3	Average
Density/(kg)m <sup>-3</sup>	1320	1400	1250	1323
Elastic modulus /MPa	4112	4133	4138	4128
Poisson's ratio	0.23	0.22	0.24	0.23
Cohesion/MPa	1.45	1.41	1.43	1.43
Internal friction Angle /(°)	20	22	24	22
Compressive strength /MPa	30	24	21	25
Coefficient of firmness f	3.0	2.4	2.5	2.6

Source: Experimental acquisition, 2020.

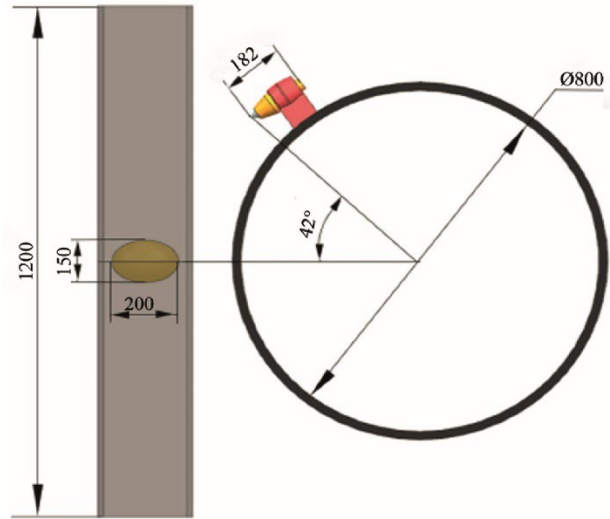


Figure 3. 3D model of single pick cuts hard concretion coal.  
Source: Simulation acquisition, 2022.

### 2.2 Establishment of hard concretion coal model

The UG tensile sketch command was used to construct a coal seam with a height of 1200mm and a drum with a diameter of 800mm. A rotary sketch was used to construct a U95 pick and an ellipsoid-shaped hard concretion with a triaxial length of 200mm×150mm×150mm, respectively. Finally, the individual parts of the structure were assembled, resulting in the 3D model of the hard concretion coal being cut by a single pick, as illustrated in Fig. 3.

## 3 Model mesh preprocessing based on Hypermesh

We imported the aforementioned 3D model in STEP format into the Hypermesh software, and used solid map to create drum mesh, and tetra mesh to obtain pick holder, pick and alloy head mesh. Then, we selected appropriate unit sizes to ensure accurate depiction of geometric features.

To analyze the stress distribution of hard concretion coal, it is necessary to consider the contact between hard concretion and coal seam in the finite element analysis. In order to analyze the internal contact between multiple parts, we treated them as a common grid. At the same time, mesh quality has a significant impact on simulation results. During the process of pick breaking of hard concretion coal and rock, the instantaneous load of the pick and the coal and rock will increase sharply when they collide, and the stress and strain of coal and rock are nonlinear, time-varying, and strongly coupled [25]. Therefore, the quality of the coal and hard concretion mesh affects the accuracy of the analysis. Traditional tetrahedral mesh has low quality, is difficult to converge, and has a large discretization error. Hexahedral grid calculations are more accurate, controllable, and less prone to negative volumes. Therefore, we divided coal and hard concretion into hexahedral grids.

To ensure accurate grid generation, the coal is initially sliced into 1/8 segments along the x, y, and z directions, followed by geometric cleaning to remove any redundant boundaries that may affect grid generation. In Hypermesh,

the mapping technique is used for hexahedral mesh division, which requires the segmented coal to be split into mapping segments. The hard concretion is initially selected according to the "from difficulty to simplicity" principle after the model analysis. The geometric model of the hard concretion body resembles an ellipsoid shape. To create the model, a cuboid is constructed with 1/4 of the length and width of the ellipsoid as its center, after which it is cut into 1/8 of the ellipsoid's size. Using the 'trim with surface' technique, a portion of the cuboid is separated from the ellipsoid's body. Next, the 1/8 ellipsoid is divided into trim nodes, as shown in Fig. 4.

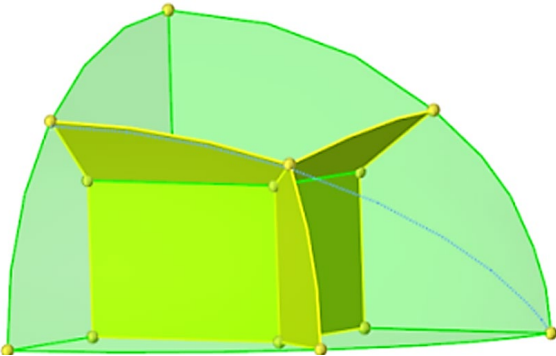


Figure 4. Mapping the one eighth ellipsoid.  
Source: Simulation acquisition, 2022.

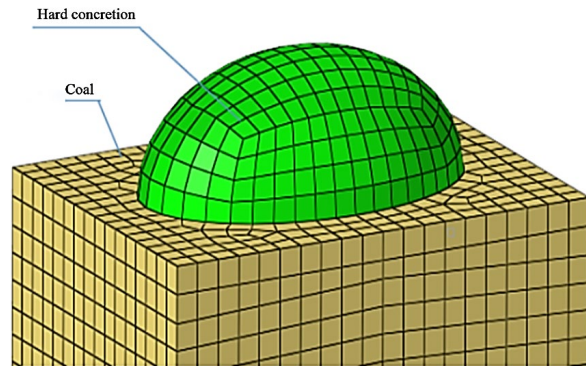


Figure 5. Meshing hard concretion coal.  
Source: Simulation acquisition, 2022.

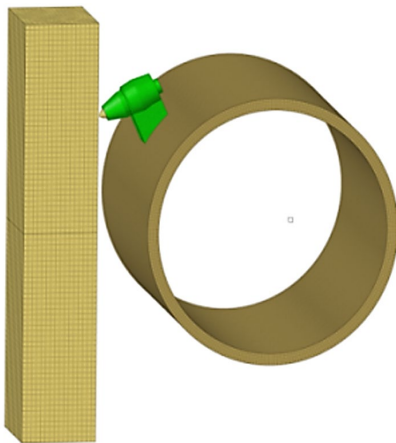


Figure 6. Model complete meshing.  
Source: Simulation acquisition, 2022.

Clicking Merge selected adjacent tetrahedral regions and merged them. Once completed, the mapped sections should be visible in the Mappable view. Then, Select the mapped sections and set the unit size to 5.0 before clicking the Mesh button. To restore 1/8 coal to the entire coal, use the Reflect button as indicated in Fig. 5. To complete the joint of coal and hard concretion, preview edges and tolerance values are selected at 0.1 of the element size.

This method results in a model comprising of 5 parts, with 200,146 nodes, and 175,408 solid elements, as illustrated in Fig. 6.

#### 4 Establishment of LS-DYNA coal-breaking simulation model

##### 4.1 Model freedom constraint setting

To ensure that the boundary nodes of the coal and hard concretion model have zero displacements in all six degrees of freedom, the \*SET\_NODE command was used to define a NODE group consisting of the two sides, upper and lower surfaces, and the back surfaces of the coal. Then, the coal boundary conditions were set on \*BOUNDRY\_SPC\_SET with 6 degrees of freedom [26].

##### 4.2 Non-reflective boundary setting

Using a fixed boundary for the coal model has a disadvantage. When the reflected stress wave reaches the fixed boundary, the coal elements are subjected to a reflected wave and a shear wave that are not consistent with the actual situation. To address this, the other five faces of the coal except for the cut face are designated as a \*segment set. Then, a non-reflective boundary condition is applied to the set node group using the \*BOUNDARY\_NON\_REFLECTING keyword to eliminate this effect.

##### 4.3 Setting of wall materials containing hard concretion

The mechanical parameters of coal and hard concretion, as listed in Tables 1 and 2, were used for the Drucker-Prager model for simulating the plastic constitutive relationship of coal wall with hard concretion [27-30].

##### 4.4 Pick type pick alloy head contact setting

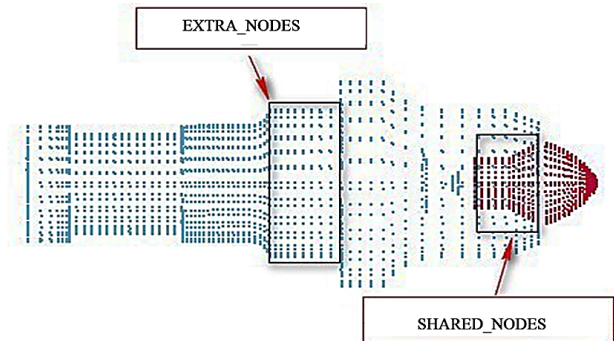


Figure 7. Shared nodes of the pick and alloy head SHARED-NODES.  
Source: Simulation acquisition, 2022.

Considering that the simulation model primarily analyzes the stress of coal, the pick holder and pick body are designated as rigid bodies, whereas the alloy head is considered a flexible body. This makes it a rigid-flexible coupling problem. The node located on the contact surface of the pick and pick holder is fixed to the pick holder using the keyword `*CONSTRAINED_EXTRA_NODES`. The common node method is used to connect the alloy head and pick body using `*SHARED_NODES`, as illustrated in Fig. 7.

#### 4.5 Contact setting of coal

In this experiment, the roller's operation efficiency was improved by attaching the pick and pick table as a rigid body. As a result, the model needs to define two contact modes: erosion contact between the pick and the hard concretion coal, and binding contact between the hard concretion and the coal. To do this, the `*CONTACT_ERODING_SURFACE_TO_SURFACE` command should be used, with the pick and coal as the primary and secondary elements, respectively. The dynamic friction coefficient for both is set to 0.01, and the static friction coefficient is set to 0.55.

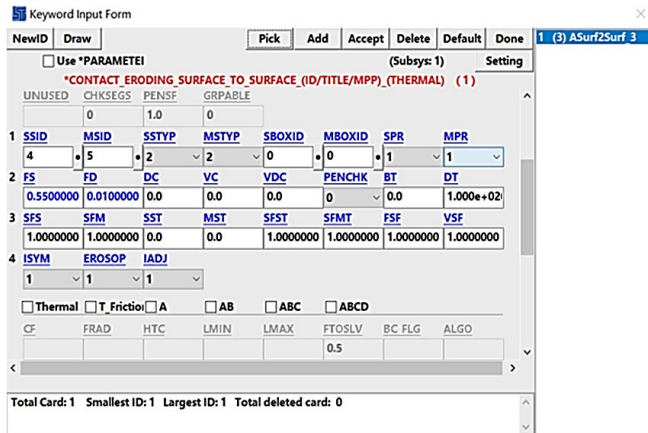


Figure 8. Related settings of the eroding surface to surface. Source: Simulation acquisition, 2022.

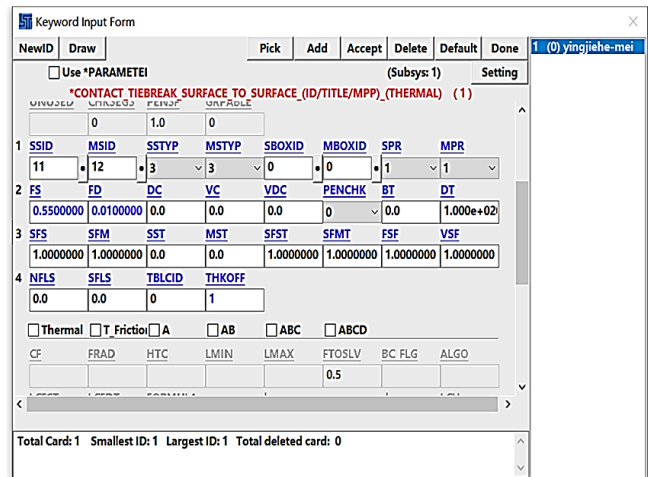


Figure 9. TIEBREAK\_SURFACE TO SURFACE settings. Source: Simulation acquisition, 2022.

To output the contact interface cloud picture of the pick, the SPR and MPR control options for the output of the master and slave slices of the contact need to be enabled. Additionally, the `*EROSOP` internal erosion option should be turned on, as shown in Fig. 8.

To account for the actual connection between coal and hard concretion, a contact between the hard concretion complex and coal is established. To do this, use the `*CONTACT_TIEBREAK_SURFACE TO SURFACE` command, with the primary element set to coal and the secondary element set to hard concretion. The `THKOFF` option should be turned on to control the offset of the surface elements, as described in [31]. The other parameter settings should be consistent with those used for the erosion contact card, as shown in Fig. 9.

#### 4.6 Setting of kinematic parameters of the roller

During actual operation, the roller should rotate and translate simultaneously. For instance, the Yanzhou Mine MG2\*70/325-BWD shearer has a drum speed of 90r/min and a traction speed of 3m/min. The `*BOUNDARY-MOTION - RIGID` command should be used to define the drum's movement and rotation speed.

#### 4.7 Output solution control

Based on the size of the hard concretion coal model and the kinematic parameters of the roller, the `*CONTROL_TERMINATION` value is set to 0.2. The energy control card is configured to include hourglass energy and slip energy calculation. To ensure accurate results, the average hourglass energy should not exceed 10% of the total energy, as recommended in [20].

### 5 Analysis of simulation results

#### 5.1 Stress variation law of coal and hard concretion

Due to the feeding speed of the shearer and the size of the pick, it was not possible to reach the back end of the hard concretion in actual working conditions. Therefore, the simulation only studied five positions of the pick acting on the front end of the long axis of the concretion body, namely 1/10, 1/5, 3/10, 2/5 and 1/2, corresponding to points A, B, C, D and E in Fig. 10.

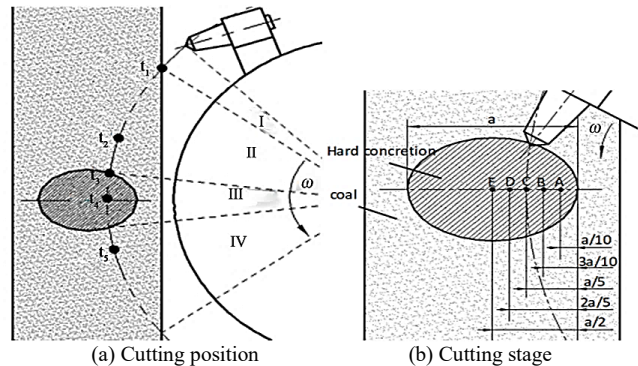


Figure 10. Pick cutting position and cutting stage. Source: Own elaboration, 2022.

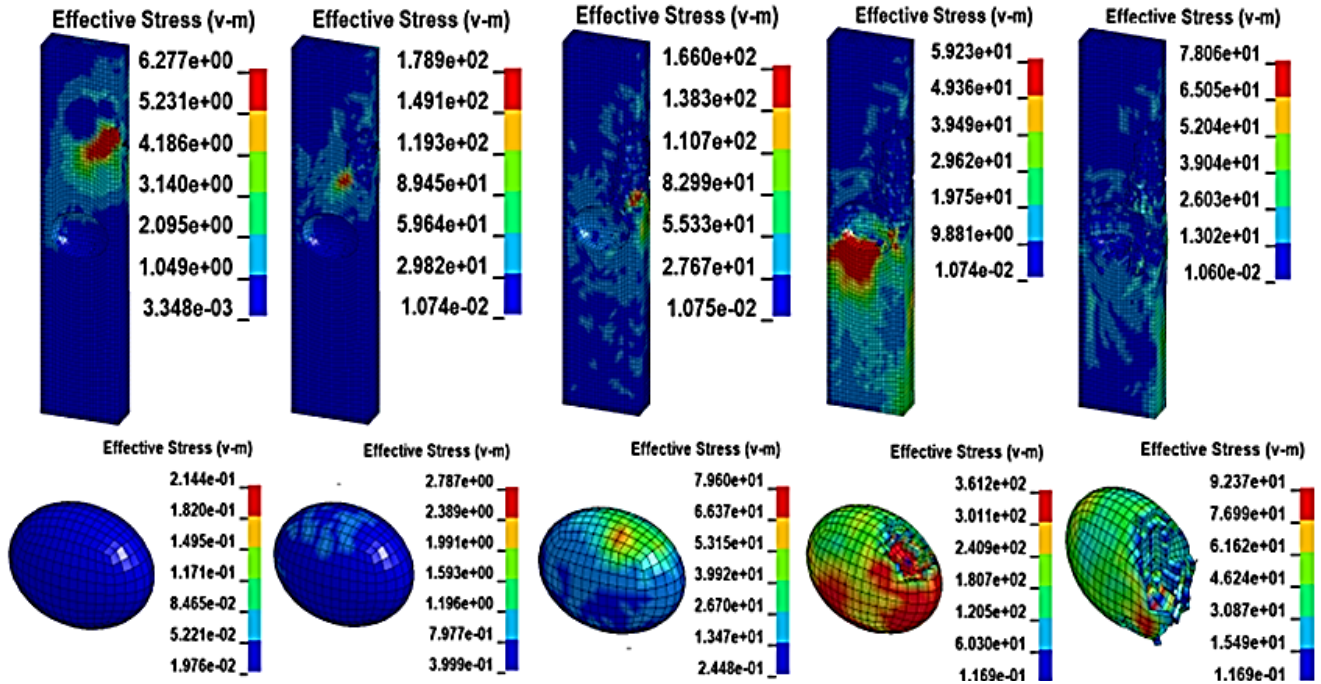


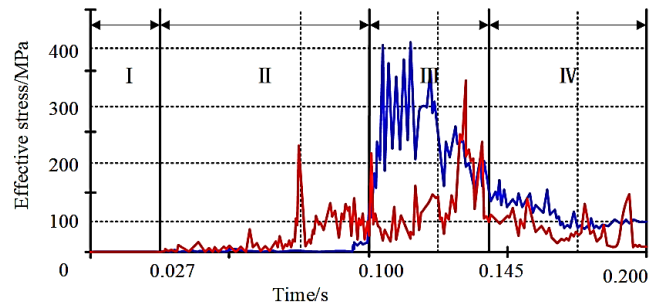
Figure 11. Effective stress cloud of coal and hard concrete. Source: Simulation acquisition, 2022.

For example, when cutting hard concrete at point C (b), click on the Effective Stress tab in the Fringe Component to view the Effective Stress cloud. At  $t_1=0.027s$ , the pick begins to cut the coal, and when the surface stress value reaches 6.277MPa stress, the element fails. At this point, the hard concrete has not been touched, so the surface stress is almost 0, as shown in Fig. 11(1). At  $t_2=0.074s$ , the pick completely enters the coal, and the local stress value reaches 178.9MPa due to the large area collapse of internal units of the coal, as shown in Fig. 11(2). At  $t_3=0.100s$ , the cutters cut above the hard concrete, and the coal unit was subjected to 166.0MPa stress. As the upper surface of hard concrete is extruded by the plastic deformation of the coal element, the hard concrete is subjected to 79.60MPa stress, as illustrated in Fig. 11(3). At  $t_4=0.115s$ , the pick acts on the inside of the hard concrete, and the maximum stress value of the coal unit is 59.23MPa due to the extrusion of the hard concrete. The hard concretions were locally broken and subjected to 86.84MPa stress, as shown in Fig. 11(4). At  $t_5=0.145s$ , the pick cuts out from the concrete body and destroys the compacted core, while the uncut hard concrete remains in the coal. At this time, the maximum stress value of the coal unit is 78.06MPa, and the maximum stress value of the hard concrete unit is 92.37MPa, as illustrated in Fig. 11(5).

Select the analysis element in the history menu and set the value to the maximum. Then, click on the coal and hard concrete to obtain the time history curve of the extreme effective stress of both materials (refer to Fig. 12). Based on the schematic diagram in Fig. 10(b) depicting the cutting stage, it can be observed that the entire cutting process can be

divided into four stages: (I) between 0s and 0.027s, the pick does not touch the coal, and the stress value remains at zero; (II) from 0.027s to 0.100s, the stress curve undergoes significant changes due to the continuous extrusion and breakage of the coal element; (III) at 0.100s, the stress curve of coal decreases while the stress value of hard concrete increases sharply because of the compacted core in the extruded coal seam; and (IV) at 0.145s, the pick is cut from the inside of the hard concrete, marking the completion of the entire cutting process at 0.200s.

Open the RCFORC item in the ASCII TAB and click on Contact1 to view the cutting force curve as depicted in Fig. 13. Once the pick started cutting the coal, the cutting force remained stable at around 20kN. As the pick entered hard concrete from coal, the cutting force experienced a sudden increase, and the maximum cutting force reached 166kN.



I - No-load stage; II - coal cutting stage; III-Cutting hard concrete stage; IV - cutting coal stage  
Figure 12. Time history curve of the maximum effective stress in the hard concrete coal. Source: Simulation acquisition, 2022.

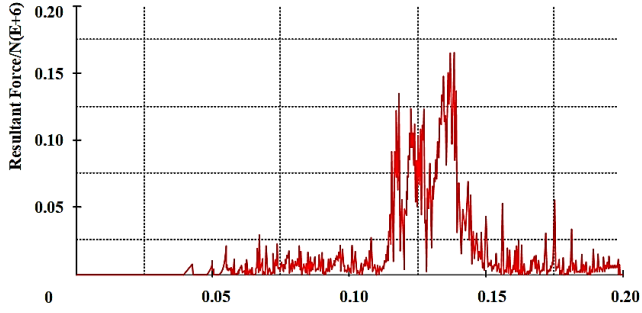


Figure 13. Cutting curve analysis at point C of hard concrete. Source: Simulation acquisition, 2022.

### 5.2 Study on the influence of cutting location parameters on coal stress peak

The coal stress cloud map was examined using d3plot, which showed that the maximum stress experienced by coal during the cutting process was 129.36MPa when cutting 1/10 of the hard concrete. Cutting 1/5 of the hard concrete resulted in a maximum stress value of 256.60MPa for coal. Cutting 3/10 of the hard concrete resulted in the maximum stress value of coal and concrete during the cutting process, which was 361.64MPa. Cutting 2/5 of the hard concrete resulted in a maximum stress value of coal during the cutting process of 659.98MPa. Cutting half of the hard concrete

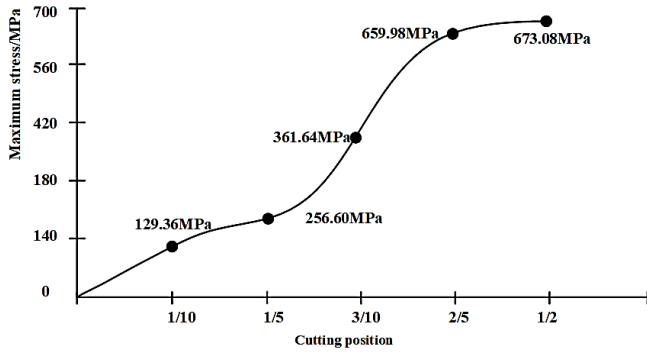


Figure 14. The maximum effective stress position of the hard concrete. Source: Simulation acquisition, 2022.

Table 3. Dimensions and related parameters of hard concrete coal.

Parameter	Symbol	Dimensional
Coal density	$\rho_m$	$ML^{-3}T^0$
Elastic modulus of coal	$E_m$	$ML^{-1}T^{-2}$
Cohesion of coal	$C_m$	$ML^{-1}T^{-2}$
Internal friction angle of coal	$\phi_m$	1
Compressive strength of coal	$\sigma_m$	$ML^{-1}T^{-2}$
Hard concrete density	$\rho_y$	$ML^{-3}T^0$
Elastic modulus of hard concrete	$E_y$	$ML^{-1}T^{-2}$
Cohesion of hard concrete	$C_y$	$ML^{-1}T^{-2}$
Internal friction angle of hard concrete	$\phi_y$	1
Compressive strength of hard concrete	$\sigma_y$	$ML^{-1}T^{-2}$
Geometry	$L$	$M^0L^1T^0$
Cutting force	$F$	$M^1L^1T^{-2}$
Gravitational force	$G$	$M^0L^1T^{-2}$

Source: Simulation experiment Acquisition, 2020.

resulted in the maximum stress value of coal during the cutting process of 673.08Ma. Based on the stress cloud map obtained, it can be seen that hard concrete will break when the pick cuts at A, B and C, while hard concrete will be cut off from coal when the pick cuts at positions D and E. Fig. 14 shows that the stress peak increases as the cutting position approaches point E (1/2) on the hard concrete.

## 6 Experimental verification

### 6.1 Deployment of hard concrete coal model based on the similarity theory

To validate the LS-DYNA simulation of the coal breaking process and uncover the accuracy of the stress variation law of hard concrete coal under pick action, a similarity model of hard concrete coal was created using the similarity theory. The physical and mechanical properties of the hard concrete coal used in the experiment were designed to be similar to those of actual coal rock by analyzing the main parameters in the MLT dimensional system, as shown in Table 3.

Based on the dimensional indices listed in Table 3, a rank 3 coefficient matrix was obtained by eliminating linearly correlated parameters:

$$\begin{bmatrix} 1 & 1 & 0 & 0 & 1 \\ -1 & -3 & 1 & 1 & 1 \\ -2 & 0 & -2 & 0 & -2 \end{bmatrix}$$

Since coal and hard concrete share the same parameters and dimensions, the basic quantity  $L$  was chosen, and the resulting dimensionless quantities are  $G, \rho, L$ .

By using Eq. (1):

$$M^{-1}L^1T^2 = (M^0L^1T^2)x_1(M^1L^{-3}T^0)x_2(M^0L^1T^0)x_3 \quad (1)$$

$x_1 = -1, x_2 = -1, x_3 = -1$  can be got.

Similarly, using Eq. (2):

$$M^{-1}L^{-1}T^2 = (M^0L^1T^2)x_1(M^1L^{-3}T^0)x_2(M^0L^1T^0)x_3 \quad (2)$$

$x_1 = -1, x_2 = -1, x_3 = -3$  can be got.

By applying the corresponding values of each parameter for hard concrete coal, the similarity criterion can be calculated using Eq. (3):

$$\pi_1 = \frac{\sigma}{G\rho L}; \pi_2 = \frac{F}{G\rho L^3} \quad (3)$$

According to the first principle of similarity, the similarity index of a similarity phenomenon is 1, and the mathematical expression of similarity coefficients can be obtained as shown in Eq. (4):

$$\frac{C_\sigma}{C_G C_\rho C_L} = 1; \frac{C_F}{C_G C_\rho C_L^3} = 1 \quad (4)$$

The geometric similarity ratio is determined based on the occurrence conditions of coal and the working environment of the project laboratory,  $C_L = 1/5$ . The material density can be controlled around  $1050 \text{ kg/m}^3 - 1100 \text{ kg/m}^3$ , so  $C_\rho = 0.83$ . According to formula (4) and the dimensional matrix, the parameters whose similarity coefficient is 0.166 are:  $\sigma_m$ ;  $\sigma_y$ ;  $E_m$ ;  $E_y$ ;  $C_m$ ;  $C_y$ . The parameters whose similarity coefficient is 0.83 are  $\rho_m$  and  $\rho_y$ , and the parameters whose similarity coefficient is 1 are  $\phi_m$  and  $\phi_y$ . The firmness coefficient  $f$  of coal and concretion mass is related to its compressive strength  $\sigma$ , and the relationship that satisfies it is indicated in Eq. (5):

$$f = \frac{\sigma}{30} + \sqrt{\frac{\sigma}{3}} \quad (5)$$

The parameters of the similar experimental coal model are shown in Table 4.

Based on the derived parameters, the ratio of sand, cement and gypsum was adjusted to 5:1.5:0.3 to simulate coal, while the ratio for simulating hard concretion was adjusted to 5:0.7:0.3. Water was then added and stirred with the material in a weight ratio of 9:1 to create the coal model, as shown in Fig. 15.

Table 4. Physical and mechanical properties of similar coal wall models.

Parameter	Unit	Prototype	Similarity Model
$\rho_m$	$\text{kg/m}^3$	1330	1104
$\sigma_m$	$\text{MPa}$	25	4
$\phi_m$	-	21	21
$E_m$	$\text{MPa}$	4118	684
$C_m$	$\text{MPa}$	4.5	0.75
$\mu_m$	-	0.2	0.2
$f_m$	-	2.5	1
$\rho_y$	$\text{kg/m}^3$	1440	1195
$\sigma_y$	$\text{MPa}$	80.7	13.4
$\phi_y$	-	48	48
$E_y$	$\text{MPa}$	14767	2451
$C_y$	$\text{MPa}$	13.6	2.3
$\mu_y$	-	0.18	0.18
$f_y$	-	8.1	2.6

Source: Simulation experiment Acquisition, 2020.

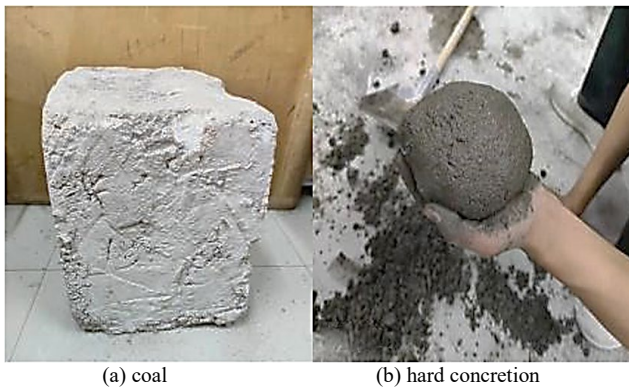


Figure 15. Model of hard concretion coal. Source: Experimental acquisition, 2022.

## 6.2 Cutting experiment verification

A cutting test bench is constructed based on the similarity principle and the requirements of the cutting experiment, as illustrated in Fig. 16. The experimental process of cutting coal that contains hard concretions using a shearer is presented in Fig. 17, while Fig. 18 shows the resulting coal model after cutting.

The experiment measured the torque curve, as shown in Fig. 19. The torque peaks during cutting of coal and hard concretion were  $T_1=2.6\text{N}\cdot\text{m}$  and  $T_2=18.6\text{N}\cdot\text{m}$ , respectively.

Based on the structural size and transmission ratio of the reducer, the peak cutting forces of the cutter for coal and hard concretion were calculated to be 141.5N and 1026.6N, respectively. According to the similarity criterion, the peak cutting force and hardening force values obtained from the cutting force curve (Fig. 13) were multiplied by the similarity coefficient of  $1.66 \times 10^5 \text{N}$  and  $2 \times 10^4 \text{N}$ , respectively, resulting in multiplication coefficients of 132.8N and 1102.2N. The relative error rate between the experiment and simulation was less than 7%. It can be concluded that LS-DYNA accurately simulated the coal breaking process and revealed the stress change rule of coal with hard concretion under the action of the pick.

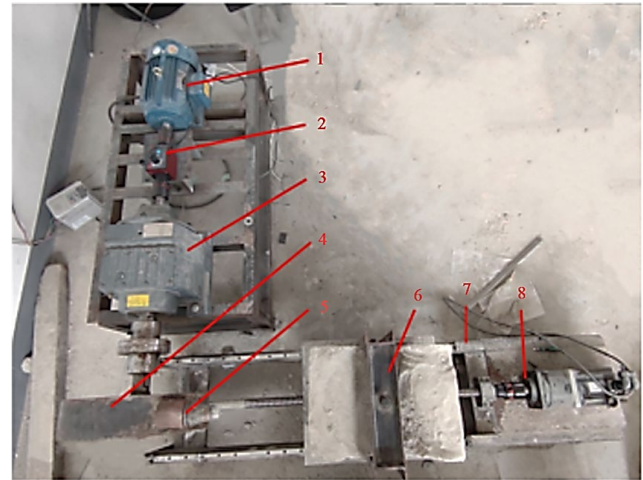


Figure 16. The composition of the experimental table. Source: Experimental acquisition, 2022.

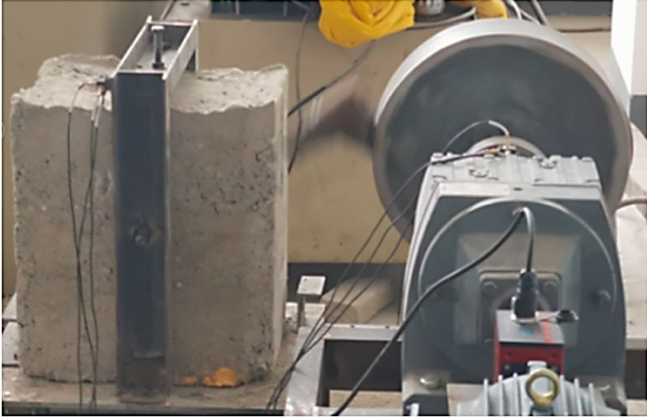


Figure 17. Experiment of cutting coal with pick.  
Source: Experimental acquisition, 2022.

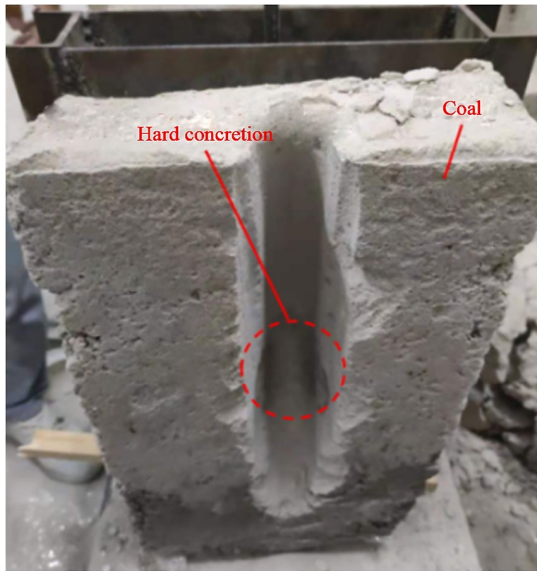


Figure 18. Model of hard concrete coal after cutting.  
Source: Experimental acquisition, 2022.

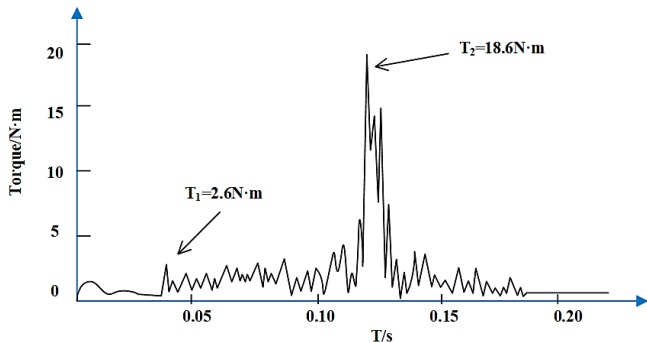


Figure 19. Reducer input torque.  
Source: Simulation acquisition, 2022.

## 7 Conclusions

1. The hexahedral mesh for the hard concrete and coal

was divided using the Hypermesh software, creating a common grid that serves as the foundation for accurately calculating the simulation model in LS-DYNA.

2. LS-PREPOST was utilized to simulate the cutting process of a single pick and reveal the stress change rules of hard concrete coal under the pick's action. Results show that when the pick is at 1/10, 1/5 and 3/10 of the long axis of hard concrete, hard concrete will break, and the coal's peak stress is 129.36MPa, 256.60MPa and 361.64 MPa respectively. When the pick is at 1/2 and 2/5 of the long axis of hard concrete, hard concrete will be cut off, and the stress peak is 659.98MPa and 673.08MPa, respectively. The closer the pick is to the center of the long axis of hard concrete, the greater the stress peak.
3. Based on the similarity theory, a coal-containing test was conducted, and an experiment was carried out on the single pick test bench. The cutting force curve obtained from the experiment was compared to the simulation results. The relative error between the two was less than 7%. Thus, LS-DYNA's ability to accurately simulate the coal breaking process is demonstrated.

## Acknowledgement

The author acknowledges the School of Mechanical Engineering and the State Key Laboratory of Mining Machinery Engineering of Coal Industry at Liaoning Technical University, China, for providing the experimental site. This work was part of a research project on "The breaking and crashing mechanism of hard concrete coal under the action of pick-shaped cutter", funded by the Education Bureau of Liaoning Province, China (grant no. LJ2019JL024), as well as a project on "Key technology and application of machine perception for industrial and mining equipment" funded by the Discipline Innovation Team of Liaoning Technical University (grant no. LNTU20TD-28). Additionally, the author would like to acknowledge another project on "Efficient thermal exploitation and utilization of new energy" funded by the Discipline Innovation Team of Liaoning Technical University (grant no. LNTU20TD-15). Finally, we would like to thank MogoEdit (<https://www.mogoedit.com>) for its English editing during the preparation of this manuscript.

## Reference

- [1] Kan, W.H., Design and research of rocker-arm of high power shearer in medium thick coal seam, MSc. Thesis, School of Mechanical and Electrical Engineering, China University of Mining and Technology, Xuzhou, Jiangsu, China, 2019, pp. 1-11. DOI: <https://doi.org/10.27623/d.cnki.gzkyu.2019.000161>
- [2] Yang SH, Zhou YC, Rui F, Development trend of thin coal seam mining and complete equipment technology, J. Coal Science and Technology, 48(03), 49-58, 2020. DOI: <https://doi.org/10.13199/j.cnki.cst.2020.03.003>
- [3] Shang, D.Y., Study on motion analysis and experiment of the inspection robot for fully-mechanized work face in thin coal seam, PhD. Thesis, College of Mechanical and Electrical Information Engineering, China University of Mining and Technology, Beijing, China, 2016, pp. 3-22.
- [4] Wang, C., Key techniques and decision support system of automatic mechanised longwall mining face in thin coal seam, PhD. Thesis,

- College of Mining Engineering, China University of Mining and Technology, Xuzhou, Jiangsu, China, 2016, pp. 1-16.
- [5] Evans, I., Basic mechanics of the point -attack, *J. Colliery Guardian*, (5), pp. 189-192, 1984.
  - [6] Evans, I., Optimum line spacing for cutting picks, *J. Mining Engineer London*, (1), art. 433, 1982.
  - [7] Wang, Q.K. and Men, Y.C., Shearer breaking theory. Coal Industry Press, 1992.
  - [8] Liu, C.S., Study on Fractal characteristics of cutting resistance curve of shearer cutter, *J. Journal of China Coal Society*, (01), pp. 115-118, 2004.
  - [9] Wang, C.H., Study on deformation and failure law of coal body under the action of cutting tooth, PhD. Thesis, Engineering Mechanics, Liaoning Technical University, Fuxin, Liaoning, China, 2004.
  - [10] Gunes, Y.N., Yurdakul, M. and Goktan, R.M., Prediction of radial bit cutting force in high-strength rocks using multiple linear regression analysis, *J. International Journal of Rock Mechanics & Mining Sciences*, 44, pp. 960-970, 2007. DOI: <https://doi.org/10.1016/j.ijrmms.2007.02.005>
  - [11] Wang, Y.N., He, Q.M. and Liu, Y.M., Development of coal and rock cutting test bed, *J. Zhongzhou Coal*, (2), pp. 9-10, 2010.
  - [12] Bakar, A., and Muhammad, Z., Evaluation of saturation effects on drag pick cutting of a brittles and stone from full scale linear cutting tests. *Tunnelling & Underground Space Technology*, 34(1), pp. 124-234, 2013. DOI: <https://doi.org/10.1016/j.tust.2012.11.009>
  - [13] Luo, C.X., Research on cutting characteristics of coal seam with coal rock interface mined by drum shearer, PhD. Thesis, School of Mechanical and Electrical Engineering, China University of Mining and Technology, Xuzhou, Jiangsu, China, 2015.
  - [14] Zhao, L.J., and Dong, M.M., Load problem of shearer working mechanism of the shearer in containing pyrites and thin coal seam, *J. Journal of China Coal Society*, 34(06), pp. 840-844, 2009.
  - [15] He, J.Q., and Wang, Z.W., Numerical simulation of coal breaking process by screw drum of thin coal seam shearer, *J. Coal Engineering*, 6, pp. 97-99, 2013.
  - [16] van Wyk, G., Els, D.N.J., Akdogan, G., Bradshaw, S.M., and Sacks, N., Discrete element simulation of tribological interactions in rock cutting, *J. International Journal of Rock Mechanics & Mining Sciences*, 65(1), pp. 8-19, 2014. DOI: <https://doi.org/10.1016/j.ijrmms.2013.10.003>
  - [17] Zhang, M.B., Stress-Damage-Seepage characteristics of coal under the influence of mining and their application, PhD. Thesis, School of Resource and Safety Engineering, China University of Mining and Technology, Beijing, China, 2015.
  - [18] Liu, X.H., Study on energy release of coal and rock crushing process under impact load, *J. Chinese Journal of Rock Mechanics and Engineering*, 6915(supp2), art. 3201, 2021.
  - [19] Zhou, W.C., Study on power transfer of shearer during coal breaking in mixed coal seam, MSc. Thesis, Liaoning Technical University, Fuxin, Liaoning, China, 2014.
  - [20] Liu, X.N., Zhao, L.J., Zhou, W.C., et al. Influence of kinematic parameters on stress of drum cutting gangue coal, *J. Journal of China coal*, 43(10), pp. 2926-2933, 2018. DOI: <https://doi.org/10.13225/j.cnki.jccs.2018.0097>
  - [21] Liu, C.S., Numerical simulation of disc tool vibration and mechanical properties of cutting and crushing coal rock, *J. Journal of Heilongjiang University of Science and Technology*, 28(01), pp. 36-42, 2018.
  - [22] Menezes, P.L., Lovell, M.R., Avdeev, I.V., and Higgs, C.F., Studies on the formation of discontinuous rock fragments during cutting operation. *International Journal of Rock Mechanics and Mining Sciences*, 71, pp. 131-142, 2014. DOI: <https://doi.org/10.1016/j.ijrmms.2014.03.019>.
  - [23] Wang, J., Analysis of tool performance and cutterhead design of pipe jacking tunneling machine for mine, MSc. Thesis, Mechanical engineering, Dalian University of Technology, Dalian, Liaoning, China, 2021. DOI: <https://doi.org/10.26991/d.cnki.gdllu.2021.002329>
  - [24] Liu, X.H., Study on interaction mechanics and wear characteristics of pick picks with coal and rock, MSc. Thesis, China University of Mining and Technology, Xuzhou, Jiangsu, China, 2016.
  - [25] Zhao, L.J., Fan, J.Y., Luo, G.H., and Wen, S.J., Reliability analysis of shearer drum vibration, *J. Journal of Vibration Engineering*, 33(01), pp. 82-87, 2020. DOI: [10.16385/j.cnki.issn.1004-4523.2020.01.009](https://doi.org/10.16385/j.cnki.issn.1004-4523.2020.01.009)
  - [26] Li, Y.C., Shi, D.Y., and Zhao, Y., Basic theory and engineering practice of ANSYS11. 0 LS-DYNA, China Water&Power Press, Beijing, 2008.
  - [27] John, O., Hallquist. LS-DYNA Keyword User's Manual, Liver more Software Technology Corporation, California, 2005.
  - [28] Li, F.Q., Research on numerical simulation technology on the breaking rock process of road header's cutting head, MSc. Thesis, Machinery manufacturing and automation, Liaoning Technical University, Fuxin, Liaoning, China, 2010.
  - [29] Bo, Y., Numerical simulation of continuous miner rock cutting process, MSc. Thesis, West Virginia University, Morgantown, WV, USA, 2005.
  - [30] Zhao, L.J., He, J.Q., and Li, F.Q., Numerical model of coal breaking process of planer Numerical simulation, *J. Journal of China Coal Society*, 2012. DOI: <https://doi.org/10.13225/j.cnki.jccs.2012.05.033>
  - [31] Liu, X.N., Zhao, L.J., Zhou, W.C., et al. Strength analysis of shearer drum cutting gangue coal rock based on LS-DYNA, *J. Journal of Mechanical Strength*, 41(06), pp. 1493-1498, 2019. DOI: <https://doi.org/10.16579/j.issn.1001.9669.2019.06.034>
- X. Liu**, received the BSc. Eng. in Mechanical Engineering and Automation in 2008, the MSc. in Mechanical Manufacturing and Automation in 2011, and the PhD in Mechanical Design and Theory in 2014, all of them from the Liaoning Technical University. Fuxin, Liaoning Province, China. Currently, he is a fully associate professor in the School of Mechanical Engineering, Liaoning Technical University. His research interests include: Modeling, dynamic simulation and control of mining machinery. Mechanical system optimization design. He hosted two provincial projects and participated in four national projects, more than 30 papers have been published. ORCID: 0000-0003-0737-2475
- Y. Zhang**, received his BSc. in Mechanical Design, Manufacturing and Automation from the Liaoning Technical University in 2019. From 2021 to now, I have studied for a master's degree in mechanical engineering at the university, focusing on modeling, dynamic simulation and control of mining machinery. ORCID: 0009-0005-3774-2723
- J. Wang**, received the BSc. Eng. in Industrial Engineering from the Liaoning Technical University in 2004, a MSc. in Mechanical Design, Manufacturing, and Automation from the Liaoning University of Technology in 2007, and a PhD. in Mechanical Design and Theory from the Liaoning Technical University in 2018. She is currently an associate professor in the School of Mechanical Engineering at the Liaoning Technical University. Her research interests include simulation, modeling of electromechanical hydraulic systems, and automation of industrial and mining equipment. ORCID: 0000-0003-3700-1261
- H. Li**, since 2020, I have studied the rigid-flexible coupling contact mode between complex geometry mesh division method and ls-dyna. During this period, I won the scholarship once, wrote one invention patent and three relevant papers, among which the dissertation was rated as an excellent graduation thesis. After graduation in 2022, I will work as a senior simulation engineer in BYD Auto Industry Co., LTD. ORCID: 0000-0001-5180-1754
- L. Ma**, is an associate researcher, received the BSc. in Mechanical Design and Automation in 2010 and a MSc. in Mechanical Manufacturing and Automation in 2013, both from the Liaoning Technical University. Since 2013, he has been engaged in the design and development of mining machinery in CCTEG Taiyuan Research Institute Co., Ltd., the main research directions include: coal mine conveying machinery design, coal mine anchoring machinery design and mine auxiliary operation robot research and development. ORCID: 0009-0003-6827-1077